

A Preliminary Report on Trace Element Determinations in Zircon and Apatite Crystals using Excimer Laser Ablation-Inductively Coupled Plasma Mass Spectrometry (ExLA-ICPMS)

Jun-Ichi Kimura*, Tohru Danhara**, and Hideki Iwano**

Abstract

We present preliminary results of micro beam trace element analysis of apatite and zircon crystals using a newly designed ArF excimer laser (193 nm DUV wave length) ablation (ExLA) coupled with a quadrupole-type high sensitivity inductively coupled plasma mass spectrometer (ICPMS). The ExLA system ablates a small amount of sample from craters 20 μm in diameter at a drilling rate of 0.125 μm per laser shot, and enables *in situ* multiple trace element analysis when coupled with ICPMS. Lower limits of detection for 28 trace elements (^7Li to ^{238}U) lie between 0.05 and 1.5 ppm, depending on sensitivity. Analyses ^{238}U and ^{232}Th in Durango standard apatite and zircons from the Osaka Group Pink Tuff show good agreement with values reported for INAA and fission track density measurements. Rare earth, large ion lithophile and high field strength elements analyses of the apatite compare well with solution-based ICPMS data. The results encourage application of the method to grain-by-grain *in situ* determination of ^{238}U in zircon or apatite, which could be used for fission track dating without irradiation in a nuclear reactor.

keywords: *excimer laser ablation, ICPMS, trace element, microanalysis, zircon, apatite*

1. Introduction

Laser ablation inductively coupled plasma mass spectrometry (LA-ICPMS) has been used successfully for determination of trace elements in rock forming minerals (Jackson *et al.*, 1992; Pearce *et al.*, 1992; Perkins *et al.*, 1992; Chen *et al.*, 1997). The method is an alternative to SIMS (secondary ion mass spectrometry) or EPMA (electron probe micro analyzer), and has been used for geological applications such as petrology and mineralogy (Gray, 1985; Jenner *et al.*, 1994; Foley *et al.*, 1996; Hirata and Nesbitt, 1997; Jeffries *et al.*, 1998; Pearce *et al.*, 1999).

LA-ICPMS is a versatile technique for microanalyses despite elemental fractionation effects in

the laser ablation process. These also occur in mass spectrometry, but to a lesser extent (Hirata and Nesbitt, 1995; Morrison *et al.*, 1995; Kimura *et al.*, 1997; Norman *et al.*, 1998, Eggins *et al.*, 1998). To overcome ablation fractionation, shorter wavelengths of laser light are preferred for minimizing thermal fractionation (Günther *et al.*, 1997; Jeffries *et al.*, 1998). Sampling efficiency is also superior with UV lasers (Günther and Heinrich, 1999a). Recently, deep UV lasers with frequency quintupled 213 nm Nd-YAG or 193 nm ArF excimer laser sources have been tested, and better ablation characteristics were obtained (Günther *et al.*, 1997; Günther and Heinrich, 1999a; Jeffries *et al.*, 1998).

Received March 20, 2000; Accepted July 15, 2000

*Department of Geoscience, Shimane University, Matsue 690-8504, Japan

**Kyoto Fission Track Co., 44-4 Minamitajima-cho, Omiya, Kita-ku, Kyoto, 603-8832, Japan

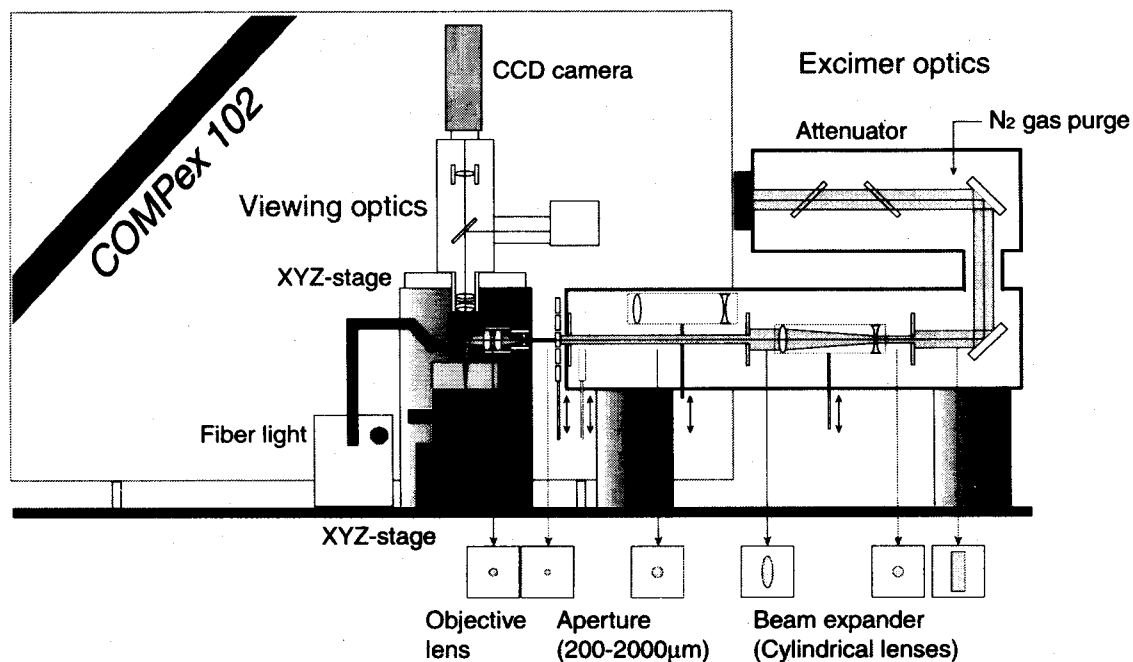


Fig. 1 Optical design of the excimer laser ablation system.

A new ArF excimer laser microprobe (ExLA) was designed and installed at the Department of Geoscience, Shimane University, and coupled with a high sensitivity quadrupole-type ICPMS. We here present preliminary results of ExLA-ICPMS analysis of zircon and apatite samples for fission track dating, and compare the analytical results for U and Th between ExLA-ICPMS and those reported INAA and by fission track methods.

2. Equipment

The excimer laser ablation (ExLA) optics used for analysis consists of Lambda Physik (Germany) COMPex 102 ArF excimer laser source and optics. The laser light source can generate 100-200 mJ pulse energy 193 nm laser light at 1-20 Hz (pulses per second; Fig.1). 193 nm UV laser light is aligned by 3 dielectric coating mirrors and is guided to a concave-convex barrel lenses beam expander. Beam divergence is adjusted for both X and Y axes for higher focusability, because excimer light source has different near-field beam divergences between X (1 mrad) and Y (3 mrad). Center part of the aligned beam is shaped by 200 μm to 1000 μm apertures depending on the ablation area required. The

masked laser beam is focused by plano-convex air-spaced doublet objective lenses with a preceding concave lens to minimize spherical aberration (Fig. 1). The laser beam is finally bounced off a coated half mirror and focused on sample surface. The viewing objective lens is set in a different light path, because it is quite difficult to use the same objective lens with UV due to difference in refractive index. A 35 mm ultra long working-distance viewing objective is used to see through the half mirror. Refraction and oblique illumination observation is available through the optics. A 0.5 mm thick half mirror is used to enable clearer on-site observation. Samples are set in a glass cell, which had a quartz window for the excimer laser. Ablation craters range from 10 to 100 μm in diameter, depending on the aperture size. Averaged drilling rate is 0.125 μm per shot at 200 mJ laser source energy, and is common for various crater sizes.

The ICPMS connected with the ExLA system is a VG Elemental (UK) VG PQ3 with S-option high efficiency expansion rotary pump. The aerosol produced from the ablation crater is transferred by Ar gas flow through the sample cell and TEFLON-

[Excimer Laser Microprobe]	
Laser source	Lambda Physik COMPex 102
Excimer gas	ArF
Wave length	193 nm
Source power	200 mJ
Repetition rate	2 Hz
Aperture	0.4 mm
Objective lens	20 X
Crater size	20 μm
Drilling rate	0.125 $\mu\text{m}/\text{shot}$
[ICP-MS]	
Instrument	VG Elemental VG PQ3 STE
S-option	ON
Expansion vacuum	0.9×10^{-6} hP
Analyzer vacuum	2.0×10^{-6} hP
Cool gas flow	13.5 l/min
Intermediate gas flow	1.1 l/min
Carrier gas flow	0.7 l/min
Cone-coil distance	5 mm
Plasma power	1350 W (forward) 0 W (reflection)

Table 1 Instrumental conditions for the ExLA microprobe and high sensitivity ICPMS.

insulated TYGON tubing, and is finally introduced into ICP. For greater ablation efficiency, He is recommended as the ablation gas (Eggins *et al.*, 1998; Günther and Heinrich, 1999b). We confirmed increased sensitivity (2-3 times) with He gas, but He was not used for this study, so we could evaluate conventional Ar gas-based properties of the system. By fine adjustment of sampling-skimmer cone distance and photon stopper allocation, this ICPMS has a high sensitivity of 400 MHz (Mcps per 1 ppm, at normal nebulization solution mode) for the ^{115}In mass peak, 250 MHz for ^{238}U and 80 MHz for ^7Li . This sensitivity is equivalent to about 500 cps/ppm for 15 mm crater and 5000 cps/ppm for 70 mm craters at a 2Hz laser repetition rate.

3. Analytical procedure

UV laser ablation was originally thought to be almost free from differing ablation efficiency between samples of different color or matrix, but actually this is not so (Eggins *et al.*, 1998; Günther and Heinrich, 1999b). We also confirmed differences in ablation

efficiency between synthetic silicate glass standard NIST SRM612 and zircon or apatite crystals. Normally, ablation efficiency is 30-50 % higher for zircon and apatite than for SRM612. Thus, the laser repetition rate for samples is set at 2 Hz, and that for the standard at 3 Hz. This sampling rate adjustment is necessary to minimize mass fractionation in ICPMS caused by space charge effect (Tanner, 1992; Kimura *et al.*, 1997). This adjustment, however, cannot fully compensate for the sampling efficiency problem, and internal standardization is thus necessary for quantitative analysis. ^{29}Si (zircon) and ^{44}Ca (apatite) were used for this purpose. Working values used for SRM612 were $\text{SiO}_2=72$ wt% and $\text{CaO}=12$ wt.% (Pearce *et al.*, 1996). Si and Ca are stoichiometric elements for zircon (ZrSiO_4) and apatite ($\text{Ca}_5[\text{PO}_4\text{CO}_3]_3[\text{F.OH.Cl}]$), respectively, and therefore these concentrations are always at constant values of $\text{SiO}_2=33$ wt.% in zircon and $\text{CaO}=55$ wt% in apatite. Analyzed SiO_2 and CaO concentrations of unknown samples are in proportion to introduced volume by laser sampling, and trace element concentrations were normalized to the ratio following the equation;

$$C_{\text{true}} = C_{\text{obs.}} \times (C(\text{Si})_{\text{stoc.}} / C(\text{Si})_{\text{obs.}}),$$

where C_{true} : true trace element concentration, $C_{\text{obs.}}$: observed trace element concentration, $C(\text{Si})_{\text{stoc.}}$: stoichiometric internal standard concentration, $C(\text{Si})_{\text{obs.}}$: observed internal standard concentration. This calculation is done off-line after nominal elemental concentration measurement.

Instrumental conditions for both ExLA and ICPMS are listed in Table 1. Source laser power was set at 200 mJ at a repetition rate of 2 or 3 Hz. The crater size used was 20 μm , and drilling rate was 0.125 μm per shot. Resulting craters were 20-25 μm in diameter, and 7-12 μm deep after 30 seconds ablation. This crater size was used as the best compromise between ExLA-ICPMS system sensitivity and spatial resolution for minerals.

Solution ICPMS analysis was also carried out on several samples using conventional standard addition method (Kimura *et al.*, 1995).

Element	612WV	AVG	2SD%	Diff%	Element	612WV	AVG	2SD%	Diff%
SiO ₂	72.00	72.00	0.0	0.0	Gd	36.95	38.28	8.0	3.6
Rb	31.63	29.55	2.7	-6.6	Tb	35.92	37.09	9.1	3.3
Sr	76.15	73.67	8.1	-3.3	Dy	35.97	34.73	7.8	-3.5
Y	38.25	39.51	11.3	3.3	Ho	37.87	38.48	8.8	1.6
Zr	35.99	33.81	14.0	-6.1	Er	37.34	37.67	6.6	0.9
Nb	38.06	41.30	5.1	8.5	Tm	37.55	37.80	7.6	0.7
Cs	41.64	43.59	7.8	4.7	Yb	39.95	37.97	9.4	-5.0
Ba	37.74	36.42	7.7	-3.5	Lu	37.71	35.72	6.9	-5.3
La	35.25	35.90	12.5	1.8	Hf	34.77	37.31	9.6	7.3
Ce	38.35	38.34	9.7	0.0	Ta	39.77	40.36	9.7	1.5
Pr	37.16	39.03	10.8	5.0	Pb	38.96	38.53	6.6	-1.1
Nd	35.24	35.30	9.3	0.2	Th	37.23	37.50	9.6	0.7
Sm	36.72	37.52	10.1	2.2	U	37.15	37.15	8.5	0.0
Eu	34.44	36.18	7.8	5.1					

Table 2 Measured NIST SRM612 values using SRM610 as the standard.

612WV: working value for SRM612 (Pearce *et al.*, 1996), AVG: average measured value for NIST612 glass. 2SD%: 2-sigma standard deviation of the analytical results. Diff%: percentage difference between working and measured values. SRM610 standard values used were from Pearce *et al.* (1996).

Element	15µm (ppm)	20µm (ppm)	50µm (ppm)	200µm (ppm)	Element	15µm (ppm)	20µm (ppm)	50µm (ppm)	200µm (ppm)
Li	1.08	0.50	0.10	0.0198	Eu	0.21	0.08	0.02	0.0033
Be	3.32	1.26	0.27	0.0504	Gd	0.38	0.16	0.03	0.0065
Rb	0.72	0.39	0.09	0.0154	Tb	0.13	0.05	0.01	0.0022
Sr	0.55	0.22	0.04	0.0089	Dy	0.42	0.17	0.03	0.0066
Y	0.72	0.30	0.05	0.0121	Ho	0.24	0.10	0.02	0.0040
Zr	2.65	1.19	0.24	0.0477	Er	0.36	0.15	0.03	0.0061
Nb	0.80	0.35	0.07	0.0139	Tm	0.06	0.02	0.00	0.0009
Cs	0.23	0.10	0.02	0.0040	Yb	0.18	0.07	0.01	0.0029
Ba	0.23	0.10	0.02	0.0039	Lu	0.09	0.04	0.01	0.0014
La	0.50	0.20	0.03	0.0081	Hf	0.69	0.29	0.05	0.0116
Ce	0.47	0.19	0.03	0.0077	Ta	0.18	0.07	0.01	0.0030
Pr	0.29	0.12	0.02	0.0048	Pb	0.69	0.28	0.06	0.0112
Nd	0.59	0.26	0.04	0.0106	Th	0.29	0.13	0.02	0.0050
Sm	1.04	0.46	0.08	0.0184	U	0.11	0.04	0.01	0.0018

Table 3 Lower limits of detection for 15, 20, and 50 µm craters at a repetition rate of 2Hz.

4. Analytical Result

4.1 Evaluation of NIST612 standards

NIST SRM612 or SRM610 glasses are the best standards available for multiple elements ExLA-ICPMS because of their overall homogeneity and existence of reliable working values (Pearce *et al.*, 1996). We normally use SRM612 as a standard because of its appropriate trace element composition. To check spatial homogeneity and relative accuracy of SRM612, we analyzed the disk using SRM610 as the standard. Deviations from the working value show 2σ errors are <10 %, and between-crater errors were also <10%. Both accuracy and homogeneity of these results are acceptable, as reported errors for working values are more or less 10 % for both 610 and 612 (Table 2).

4.2 Lower limits of detection

Lower limits of detection (LLD) were determined by measuring gas blanks 10 times under normal measuring conditions. Element sensitivity was determined using NIST SRM612 with 20 µm craters at 2Hz repetition rate. LLD was then calculated by 3σ deviation of background element concentrations, and was 0.01-2 ppm depending on element sensitivity. This LLD range is adequate for the concentrations of most trace elements in zircon and apatite (Table 3).

4.3 Durango apatite

We analyzed Durango apatite, which is used as an standard for fission track dating method (Naeser *et al.*,

Element	DA1(LA)	1SD	Remarks	DA2(LA)	1SD	Remarks	DA1(SOL)	Diff%
CaO	55.	-		55.	-		-	-
Rb	.1	.32		.33	.3		.11	-2.5
Sr	527.	18.		516.	10.		472.	11.7
Y	544.	23.		419.	13.		552.	-1.4
Zr	.48	.36	LLD	.61	.6	LLD	1.3	-
Nb	.05	.05	LLD	.07	.11	LLD	.01	-
Cs	.04	.04	LLD	.03	.04	LLD	-	-
Ba	1.62	.29		1.85	.3		-	-
La	3444.	335.	SAT	3299.	89.	SAT	4195.	-
Ce	2626.	566.	SAT	2710.	382.	SAT	4427.	-
Pr	378.	29.		362.	11.		379.	-0.3
Nd	1064.	84.		1051.	52.		1121.	-5.1
Sm	143.	9.		126.	3.		147.	-2.7
Eu	16.2	1.		16.4	.4		16.5	-1.8
Gd	191.	22.		171.	5.		163.	17.2
Tb	17.4	1.13		13.7	.4		18.1	-3.9
Dy	96.9	5.23		76.3	2.1		102.	-5.0
Ho	17.4	1.67		13.9	.4		18.6	-6.5
Er	49.9	2.9		38.2	1.		48.3	3.3
Tm	6.29	.31		4.7	.2		6.2	1.4
Yb	33.7	2.		27.1	.6		35.2	-4.3
Lu	4.2	.3		3.8	.1		4.4	-4.5
Hf	.06	.06	LLD	.05	.05	LLD	.11	-
Ta	.01	.01	LLD	.02	.03	LLD	.04	-
Pb	1.4	.82		1.6	1.2		-	-
Th	253.	24.		162.	4.		256.	-1.2
U	12.5	1.2		7.5	.3		13.8	-9.4

	INAA1	INAA2	FTD-A	FTD-B	FTD-C
Th	162 (2)	183 (2)	-	-	-
U	7.6 (1.2)	7.9 (1.1)	10.2 (0.3)	12.9 (0.3)	15.7 (0.3)

Table 4 ExLA-ICPMS analysis of Durango apatite.

Measured results are normalized to CaO = 55 wt.%. DA1 and DA2: flakes 1 and 2. 1SD: 1 sigma standard deviation. LLD: below lower limit of detection, SAT: above detector saturation range. DA1 measured by ExLA method shows excellent agreement with solution analysis of the same sample. DA2 U and Th results show good agreement with published INAA analyses (Honda *et al.*, 1980). The U range from ExLA compares well with U contents measured by induced fission track density (FTD-A to -C, Danhara and Iwano unpublished data).

1979). Two flakes of apatite were first measured with ExLA-ICPMS for Rb, Sr, Y, Zr, Ba, Cs, REE, Hf, Ta, Pb, Th, and U. More than twenty spots were analyzed to cover the entire exposed surface, to average any crystal heterogeneity. The largest apatite flake was then removed from its mount and weighed on a high precision electric balance. Weighing was repeated 20 times, the highest and lowest values discarded, and the average value then calculated. The flake was then

dissolved in 6N HCl, 1 ppb equivalent ¹¹⁵In internal standard added, and the solution diluted 200000 times. This solution was then measured by conventional solution ICPMS.

The ExLA-ICPMS and solution- ICPMS results show very good agreement (flake DA1, Table 4), except for Pb and Ba, which were extremely high value in the solution ICPMS analyses. This proved to be due to contamination from the glue used for the crystal

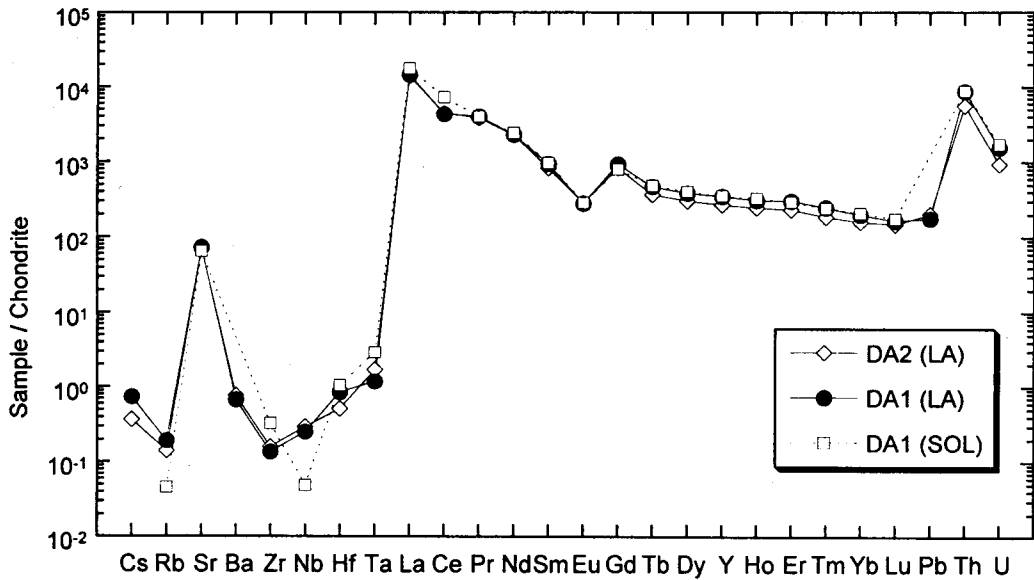


Fig. 2 Chondrite normalized element abundances of Durango apatite. DA1 (LA): flake 1 by laser ablation. DA2 (LA): flake 2 by laser ablation. DA1 (SOL): solution analysis of flake 1. Normalizing values from Taylor and McLennan (1985). Excellent agreement is shown between ExLA and solution results for flake 1, except for elements below LLD (Zr to Ta) and for those with detector saturation (La and Ce). HREE, Th and U in flake 2 are systematically lower than in flake 1, suggesting Durango apatite is heterogeneous.

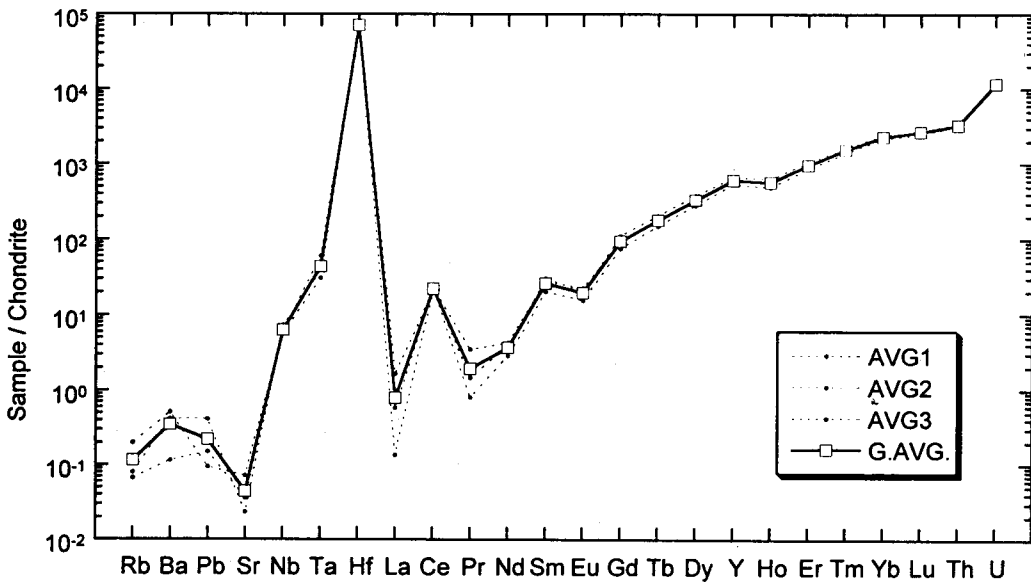


Fig. 3 Chondrite normalized element abundances of OGPK zircons. AVG1 to 3: averaged value of 3 batches of 20 zircon crystals. G.AVG.: grand average. Variations in REE, HFSE, Th and U are small, suggesting a homogeneous magma origin. Rb, Ba, Pb and Sr are close to LLD.

mount, and results of the two elements were subsequently discarded. Quite large discrepancies were also seen for La and Ce. This was due to high count rates by ExLA (> 2.5Mcps), which caused saturation of

the PC (proportional counter) detector. The low results for these elements by ExLA are consistent with counting losses at high count rates. Zr, Hf, Ta, Nb are below LLD in laser ablation, but the averages from 20

spots generally agree well with the results from solution. These elements apart, the ExLA results agree within error ($\pm 5\%$, mainly from weighing error) with the solution results, showing that the ExLA results are accurate and matrix effects for apatite are small (Figs. 2 and 3).

Uranium contents from INAA, fission track, and ExLA-ICPMS show generally good agreement, although U, Th and HREE contents of different blocks of Durango apatite differ. Flake DA1 was checked by solution ICPMS as noted above. Flake DA2 has an average U content of 7.8 ppm, which compares well with bulk INAA results ($U = 7.8$ ppm, (Honda *et al.*, 1980)). The INAA result for another block is 9 ppm, comparable with that U content determined by induced fission track density ($U = 10.2-15.7$ ppm; FTD-C: Danhara and Iwano this volume). When the highest U content ($U = 12-13$ ppm) from DA1 is also considered, the Durango apatite has U content ranging from 7.8 to 15.7 ppm. Contents in single apatite flakes (DA1 and DA2) also vary between 6 to 15 ppm, suggesting in-flake heterogeneity. Precise correlation of individual apatite block between the methods is thus not possible. However, average U contents measured by the three different analytical methods agree overall, demonstrating that ExLA-ICPMS method is a versatile technique for quantitative analysis of U, provided a sufficient numbers of measurements are made.

4.4 OGPK zircon

Zircon crystals have long been used for fission track dating due to their high U contents, their resistance to weathering, and because they are common constituents of acid igneous rocks. Zircons are silicates, but differ in Zr and Hf contents. Zircon analyses by LA-ICPMS using 266 nm UV Nd-YAG laser have been reported, and generally show 'reasonable' results (Jackson *et al.*, 1992; Pearce *et al.*, 1992; Perkins *et al.*, 1992). However, comprehensive evaluation of trace element concentrations in zircon is not yet complete. It is known that element concentrations vary widely between crystals, and therefore has been difficult to find homogeneous zircons even for standard samples.

Element	OGPK1	OGPK2	OGPK3	G.AVG.	1SD
SiO ₂	33.00	33.00	33.00	33.00	-
Rb	0.28	0.16	0.16	0.20	0.07
Sr	0.44	0.26	0.16	0.29	0.14
Y	961	1036	846	948	96
Nb	1.47	1.40	1.75	1.54	0.18
Ba	0.77	0.28	0.90	0.65	0.33
La	0.36	0.03	0.11	0.17	0.17
Ce	13.8	13.2	13.9	13.6	0.3
Pr	0.31	0.14	0.07	0.17	0.12
Nd	1.85	1.81	1.34	1.67	0.28
Sm	4.25	4.67	3.14	4.02	0.79
Eu	1.32	1.18	0.90	1.14	0.21
Gd	19.8	22.9	15.8	19.5	3.5
Tb	6.81	7.75	5.69	6.75	1.03
Dy	84.9	96.4	73.0	84.8	11.7
Ho	32.5	35.4	28.3	32.1	3.6
Er	157	174	144	158	15
Tm	40.3	41.8	35.8	39.3	3.1
Yb	388	411	371	390	20
Lu	71.2	70.7	62.7	68.2	4.8
Hf	7496	7013	8074	7528	531
Ta	0.85	0.43	0.54	0.60	0.22
Pb	0.14	0.34	0.84	0.44	0.36
Th	91.9	99.9	97.0	96.3	4.1
U	90.2	89.4	98.7	92.7	5.2

Table 5 ExLA-ICPMS analytical results for the OGPK zircons. Measured results are normalized to SiO₂ = 33 wt.%. OGPK1 to 3: zircons from the Pink Ash of the Osaka Group, G.AVG.: grand average, 1SD: 1 sigma standard deviation in grand total. Measured U content of OGPK zircon (93 ± 5 ppm) show good agreement of that measured by induced fission track density (99 ± 11 ppm; Danhara *et al.*, 1997).

The Pink Ash in the Plio-Pleistocene Osaka Group (OGPK) is a widespread co-ignimbrite rhyolitic tephra (Kamata *et al.*, 1997). Zircon crystals in the OGPK are found to be relatively homogeneous in color, shape, and U contents among samples (Danhara *et al.*, 1997). OGPK zircons were analyzed by ExLA-ICPMS analysis to evaluation chemical homogeneity. Each grain was analyzed with 60 shots of laser pulses resulted in 7.5 μ m depth craters. Analyses of three batches of 20 randomly selected zircon grains show good agreement in averaged U content (89 to 99 ppm). This range is within that determined by induced fission track density (99 ± 11 ppm; (Danhara *et al.*, 1997))

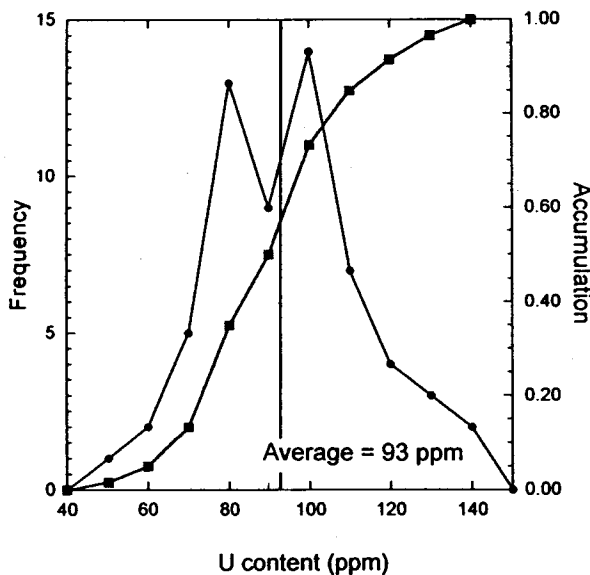


Fig. 4 Histogram showing U contents of individual OGPK zircons. Average value is 93 ppm and compositional variation ranges from 65 to 125 ppm. Histogram shows almost Poisson distribution.

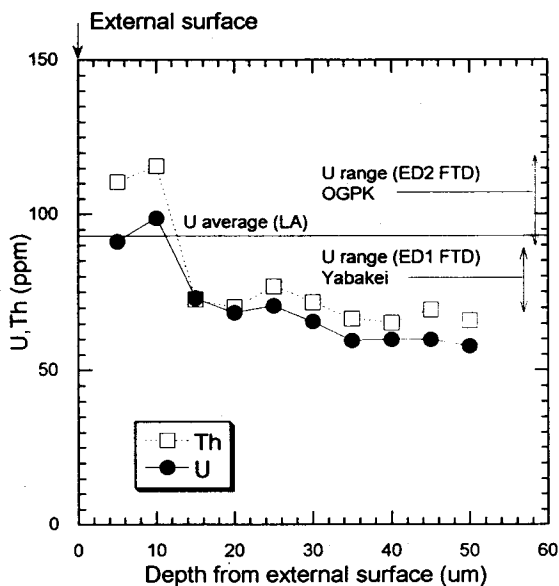


Fig. 5 U-Th depth profiles of OGPK zircon. A thin (10 μm) high-U, high-Th rim surrounds a relatively uniform core. Rim compositions are comparable with averaged OGPK U and Th contents determined by ExLA from 20 μm diameter craters 15-20 μm deep. The entire range of U is consistent with U variations from 2π and 4π surfaces determined by induced fission track density measurements (Danbara and Iwano, unpublished data).

(Table 5). U contents in single grains vary from 65 to 125 ppm. A histogram of all 60 results shows a Poisson distribution (Fig. 4). Besides this general agreement in U content, REE and HFSE contents of single zircons fall within a narrow range, suggesting they are homogeneous.

To confirm within-grain variation (chemical zoning), vertical Th and U concentration profiles in a single zircon crystal were analyzed. For this purpose, data acquisition time was set at consecutive 10 seconds intervals, with continuous 4Hz laser ablation up to 90 seconds. This setup acquires element concentrations for each ca. 5 μm depth, and gives a down-hole element profile 45 μm deep. The Th and U profiles show high concentrations in the 5-10 μm at the rim, and decrease sharply between 10 and 20 μm , before leveling out into the core between 25 to 45 μm . U contents in rim and core are 95 ppm and 60 ppm, respectively, consistent with U contents measured by fission track density in external 2π (U = 90-110 ppm) and internal 4π (U = >70 ppm) surfaces (Fig. 5, (Danbara *et al.*, 1997)). Similar zoning was found in all zircons examined. We conclude that the OGPK zircon crystallized from the host rhyolitic magma in equilibrium conditions at least in the rims. General agreements for U contents between fission track based methods and ExLA-ICPMS shows the potential of ExLA for direct U measurement of zircons with a spatial resolution of 20 μm and depth of 5-10 μm .

Comparison between solution and ExLA ICPMS of OGPK zircons is necessary for further evaluation of the versatility of ExLA-ICPMS using NIST SRM612 as the standard. We are now conducting ICPMS measurement utilizing alkali fusion after acid digestion to test the methodology further. Results will be given in a separate paper.

5. Summary

Preliminary results of ExLA-ICPMS analysis of Durango apatite and OGPK zircons show excellent to good agreements with solution based ICPMS and INAA or fission track U contents. The results clearly

indicate that quantitative ExLA-ICPMS analysis of U and other trace elements in zircon and apatite can be carried out successfully. The results also show that NIST SRM612 silicate glass can be used as a standard, and that matrix effects between the silicate standard and apatite or zircon are not significant in ExLA-ICPMS analysis. However, quantitative U analysis for age determination requires accuracy and precision better than 1%.

Further evaluation of the method is being carried out using both solution and ExLA-ICPMS, and a comprehensive report of the versatility and applicability of ExLA-ICPMS will be given in a further paper. However, the results suggest that high spatial resolution, precision, and sensitivity of ExLA-ICPMS make the method well suited for evaluating mineral heterogeneity, and may also permit fission track dating without neutron irradiation.

Acknowledgements

We thank Profs. D. Günther (ETH Zurich), N.J.G. Pearce (Wells University), T. Honda (Musashi Technology University), M. Hayashi (Kyushu Industrial University), and Dr. H. Ohira (Shimane University), for discussions, and Dr. B. Roser (Shimane University) for his comments on the manuscript. Mr. K. Ohki of the OK Laboratory Limited constructed the ExLA optics. This work was supported by Grant-in-Aid nos. 10304038 (Rep. Kimura J. -I.), 10440150 (Rep. Takasu A.), 11640454 (Rep. Sano S.) from the Ministry of Education, Science, Sports, and Culture, and funding from the Technical Research Center of the Japan National Oil Cooperation, project "Estimation of Sediments Sources, Depositional Environments, and Diagenesis of Oil Source Rocks Using Trace and Ultra-trace Elements".

References

Chen, Z., Doherty, W. and Gregorie, D.C., 1997, Application of laser sampling microprobe inductively coupled plasma mass spectrometry to in situ trace element analysis of selected geological materials. *Jour. Anal. Atom. Spectrom.*, **12**, 653-659.

- Danhara, T., Kamata, H. and Iwano, H., 1997, Fission track ages of zircons in the Yabakei pyroclastic-flow deposit in Kyushu and the Oink Volcanic Ash of the Osaka Group. *Jour. Geol. Soc. Japan*, **103**, 994-997 (in Japanese with English abstract).
- Eggins, S.M., Kinsley, L.P.J. and Shelley, J.M.G., 1998, Deposition and element fractionation processes during atmospheric pressure laser sampling for analysis by ICP-MS. *Appl. Surf. Sci.*, **127-129**, 278-286.
- Foley, S.F., Jackson, S.E., Fryer, B.J., Greenough, J.G. and Jenner, G.A., 1996, Trace element partition coefficients for clinopyroxene and phlogopite in an alkaline lamprophyre from Newfoundland by LAM-ICP-MS. *Geochim. Cosmochim. Acta*, **60**, 629-638.
- Gray, A.L., 1985, Solid sample introduction by laser ablation for inductively coupled plasma source mass spectrometry. *Analyst*, **110**, 551-556.
- Günther, D., Frischknecht, R., Heinrich, C.A. and Kahlert, H.-J., 1997, Capabilities of an ArF 193 nm excimer laser for LAM-ICP-MS micro analysis of geological materials. *Jour. Anal. Atom. Spectrom.*, **12**, 939-944.
- Günther, D. and Heinrich, C.A., 1999a, Comparison of the ablation behavior of 266 nm Nd:YAG and 193 nm ArF excimer lasers for LA-ICP-MS analysis. *Jour. Anal. Atom. Spectrom.*, **14**, 1369-1347.
- Günther, D. and Heinrich, C.A., 1999b, Enhanced sensitivity in laser ablation-ICP mass spectrometry using helium-argon mixtures as aerosol carrier. *Jour. Anal. Atom. Spectrom.*, **14**, 1363-1368.
- Hirata, T. and Nesbitt, R.W., 1995, U-Pb isotope geochemistry of zircon: Evaluation of the laser probe-inductively coupled plasma mass spectrometry technique. *Geochim. Cosmochim. Acta*, **59**, 2491-2500.
- Hirata, T. and Nesbitt, R.W., 1997, Distribution of platinum group elements and rhenium between metallic phases of iron meteorites. *Earth Planet. Sci. Lett.*, **147**, 11-24.
- Honda, T., Danhara, T. and Nozaki, T., 1980, U and Th contents in standard materials for fission track dating

- and their effects to zeta-value. *Fission Track Newslett.*, **3**, 28-35 (in Japanese with English abstract).
- Jackson, S.E., Longerich, H.P., Dunning, G.R. and Fryer, B.J., 1992. The application of laser-ablation microprobe-inductively coupled plasma-mass spectrometry (LAM-ICP-MS) to in situ trace-element determination in minerals. *Canad. Mineral.*, **30**, 1049-1064.
- Jeffries, T.E., Jackson, S.E. and Longerich, H.P., 1998, Application of a frequency quintupled Nd:YAG source ($r=213$ nm) for laser ablation inductively coupled plasma mass spectrometric analysis of minerals. *Jour. Anal. Atom. Spectrom.*, **13**, 935-940.
- Jenner, G.A., Foley, S.F., Jackson, S.E., Green, T.H., Fryer, B.J., and Longerich, H.P., 1994, Determination of partition coefficients for trace elements in high pressure-temperature experimental run products by laser ablation microprobe-inductively coupled plasma-mass spectrometry (LAM-ICP-MS). *Geochim. Cosmochim. Acta*, **58**, 5099-5103.
- Kamata, H., Hayashida, A. and Danhara, T., 1997. Identification of a pair of co-ignimbrite ash and underlying distal plinian ash in the lower Pleistocene widespread tephra in Japan. *Jour. Volc. Geotherm. Res.*, **78**, 51-64.
- Kimura, J.-I., Tsuchiya, N., Sano, S., Chuman, N. and Yoshida, T., 1997, Quantitative trace element analysis using inductively coupled plasma-mass spectrometry (ICP-MS). *Chikyu-Kagaku*, **31**, 133-151 (in Japanese with English abstract).
- Kimura, J.-I., Yoshida, T. and Takaku, Y., 1995, Igneous rock analysis using ICP-MS with internal standardization, isobaric ion overlap correction, and standard addition methods. *Sci. Rep. Fukushima Univ.*, **56**, 1-12.
- Morrison, C.A., Lambert, D.D., Morrison, R.J.S., Ahlers, W.W. and Nicholls, I.A., 1995, Laser ablation-inductively coupled plasma-mass spectrometry: an investigation of elemental responses and matrix effects in the analysis of geostandard materials. *Chem. Geol.*, **119**, 13-29.
- Naeser, C.W., Gleadow, A.J.W. and Wagner, G.A., 1979, Standardization of fission track data reports. *Nucl. Tracks*, **3**, 133-136.
- Norman, M.D., Griffin, W.L., Pearson, N.J., Garcia, M.O. and O'Reilly, S.Y., 1998, Quantitative analysis of trace element abundances in glasses and minerals: a comparison of laser ablation inductively coupled plasma mass spectrometry, solution inductively coupled plasma mass spectrometry, proton microprobe and electron microprobe data. *Jour. Anal. Atom. Spectrom.*, **13**, 477-482.
- Pearce, N.J.G., Perkins, W.T., Abell, I., Duller, G.A.T. and Fuge, R., 1992, Mineral microanalysis by laser ablation inductively coupled plasma mass spectrometry. *Jour. Anal. Atom. Spectrom.*, **7**, 53-57.
- Pearce, N.J.G., Perkins, W.T., Westgate, J.A., Gorton M.G., Jackson, S.E., Near, C.R., and Chenery, S.P., 1996, A compilation of new and published major and trace element data for NIST SRM610 and NIST SRM612 glass reference materials. *Geost. Newslett.*, **21**, 115-144.
- Pearce, N.J.G., Westgate, J.A., Perkins, W.T., Eastwood, W.J. and Shane, P., 1999, The application of laser ablation ICP-MS to the analysis of volcanic glass shards from tephra deposits: bulk glass and single shard analysis. *Glob. Planet. Change*, **21**, 151-171.
- Perkins, W.T., Pearce, N.J.G. and Fuge, R., 1992, Analysis of zircon by laser ablation and solution inductively coupled plasma mass spectrometry. *Jour. Anal. Atom. Spectrom.*, **7**, 611-616.
- Tanner, S.D., 1992, Space charge in ICP-MS: calculation and implications. *Spectrochim. Acta*, **47B**, 809-823.
- Taylor, R.S. and McLennan S.M., 1985, The continental crust: its composition and evolution. Blackwell Scientific, London, pp. 312.